PLOS ONE

RESEARCH ARTICLE

Longitudinal Changes in White Matter Tract Integrity across the Adult Lifespan and Its Relation to Cortical Thinning

Andreas B. Storsve[1]*, Anders M. Fjell[1,2], Anastasia Yendiki[3], Kristine B. Walhovd[1,2]

1 Research Group for Lifespan Changes in Brain and Cognition, Department of Psychology, University of Oslo, 0373, Oslo, Norway, **2** Department of Physical Medicine and Rehabilitation, Unit of Neuropsychology, Oslo University Hospital, 0424, Oslo, Norway, **3** Athinoula A. Martinos Center for Biomedical Imaging, Department of Radiology, Massachusetts General Hospital and Harvard Medical School, Boston, MA, United States of America

* a.b.storsve@psykologi.uio.no

Citation: Storsve AB, Fjell AM, Yendiki A, Walhovd KB (2016) Longitudinal Changes in White Matter Tract Integrity across the Adult Lifespan and Its Relation to Cortical Thinning. PLoS ONE 11(6): e0156770. doi:10.1371/journal.pone.0156770

Editor: Klaus Ebmeier, University of Oxford, UNITED KINGDOM

Received: January 14, 2016

Accepted: May 19, 2016

Published: June 2, 2016

Data Availability Statement: Ethical restrictions imposed by the Regional Committee for Medical and Health Research Ethics (REC South East Norway) as well as data storage requirements in accordance with Norwegians Laws of privacy protection does not allow for public availability of participant data. However, anonymized data will be made available upon request to all interested researchers, pending ethical approval from REC. Interested researchers may contact project leader Prof. Kristine B. Walhovd (k.b.walhovd@psykologi.uio.no), who will seek permission to share this data.

Abstract

A causal link between decreases in white matter (WM) integrity and cortical degeneration is assumed, but there is scarce knowledge on the relationship between these changes across the adult human lifespan. We investigated changes in thickness throughout the cortical mantle and WM tract integrity derived from T1 and diffusion weighted magnetic resonance imaging (MRI) scans in 201 healthy adults aged 23–87 years over a mean interval of 3.6 years. Fractional anisotropy (FA), mean (MD), radial (RD) and axial (AD) diffusivity changes were calculated for forceps minor and major and eight major white matter tracts in each hemisphere by use of a novel automated longitudinal tractography constrained by underlying anatomy (TRACULA) approach. We hypothesized that increasing MD and decreasing FA across tracts would relate to cortical thinning, with some anatomical specificity. WM integrity decreased across tracts non-uniformly, with mean annual percentage decreases ranging from 0.20 in the Inferior Longitudinal Fasciculus to 0.65 in the Superior Longitudinal Fasciculus. For most tracts, greater MD increases and FA decreases related to more cortical thinning, in areas in part overlapping with but also outside the projected tract endings. The findings indicate a combination of global and tract-specific relationships between WM integrity and cortical thinning.

Introduction

Cortical gray matter (GM) and underlying white matter (WM) are by theoretical accounts assumed to change in synchrony [1, 2]. GM damage is expected to lead to WM degeneration, e.g. through Wallerian degeneration [2], where degeneration of axons separated from their cell bodies is seen followed by slower degradation of the myelin sheath. And vice versa, WM damage has adverse effects on neuronal functioning [3]. However, there is currently little empirical evidence to support a relation between cortical GM and WM changes at a structural level[4]. This is so despite established consensus that marked brain changes in both GM and WM

Funding: This work was supported by the Department of Psychology, University of Oslo (A.B.S., K.B.W.), the Norwegian Research Council (to K.B.W., A.M.F.), the European Research Council's Starting Grant scheme (Grant 313440 to K.B.W. and Grant 283634 to A.M.F.), the US-Norway Fulbright Foundation (to A.B.S.), the National Institute for Biomedical Imaging and Bioengineering (R00-EB008129, R01-EB006758) (to A.Y.) and the National Institutes of Health Blueprint for Neuroscience Research (5U01-MH093765) (to A.Y.), part of the multi-institutional Human Connectome Project. Additional resources were provided by the Center for Functional Neuroimaging Technologies, P41EB015896, a P41 Biotechnology Resource Grant supported by the National Institute of Biomedical Imaging and Bioengineering, National Institutes of Health (to A.Y.). This work also involved the use of instrumentation supported by the NIH Shared Instrumentation Grants S10RR023401, S10RR019307, S10RR019254, S10RR023043. The funders had no role in study design, data collection and analysis, decision to publish, or preparation of the manuscript.

Competing Interests: The authors have declared that no competing interests exist.

normally take place throughout adulthood [5–13]. While monotonically decreasing age trajectories are typically observed for regional cortical thinning, WM macro-and microstructure is reported to show an inverse U-shaped age trajectory, with volume growth and maturational processes in terms of increases in directionality of diffusion appearing to plateau around the age of 30 [13–15]. Although differing trajectories are observed in development and younger adulthood, MRI studies of both cortical GM [12, 14, 16–18] and WM [15] point to accelerated changes in select regions after the age of 60. Multimodal imaging studies have revealed widespread age-related differences in multiple tissues and parameters [19, 20]. However, the specific relation between cortical GM changes and changes in underlying WM tracts has to our knowledge never been investigated longitudinally. Recently, we quantified cortical GM [12] and WM diffusion [13] changes in the adult lifespan across a 3.6 year period. In the current study, we quantify longitudinal WM tract changes using a new method, which is a longitudinal extension of TRActs Constrained by UnderLying Anatomy (TRACULA) [21, 22]. We investigate whether and how changes in WM measures at the level of individual tracts relate to previously reported changes in cortical thickness [12] within the same time period.

Besides giving tract-specific information, the current analysis approach is particularly well suited to map the relationship between macrostructural cortical changes and diffusivity changes in the WM fascicles, as the algorithm for automated probabilistic tractography relies on the anatomical information of each individual [21, 22]. We recently performed a voxel-based analysis on longitudinal data from this cohort, using tract-based spatial statistics (TBSS), and found extensive and overlapping annual decreases in WM fractional anisotropy (FA), and increases in axial (AD), radial (RD) and mean diffusivity (MD) [13]. Spatially, results were consistent with inferior-to-superior gradients of lesser-to-greater vulnerability. Annual change increased with age, particularly within superior regions, with age-related decline estimated to begin in the fifth decade [13]. However, the observed gradients of magnitude of change in this study did not map directly on to specific tracts. As recently reviewed by Bennett and Madden [23], relatively little is known of the tract-specificity of normal WM age changes. A global effect of age on WM integrity has been observed in diffusion imaging data [24], while tract-specific effects have also been identified [25, 26]. In a recent study of individual variation in WM and perceptual motor speed in younger and older adults, which included the genu and splenium of the corpus callossum, superior longitudinal fasciculi and the corticospinal tract, influences beyond the level of individual tracts were indicated, but the extent to which regional or global effects predominated differed across measures [27]. More regional effects were observed for FA in superior longitudinal fasciculi, corticospinal tracts and optic radiations, while for MD, RD, and AD primarily global, brain-general variation was observed [27].

To the extent that there are global effects of age on microstructural WM changes, and widespread cortical changes in aging, it might not be realistic to expect highly specific relations with cortical changes either. In one smaller-scale clinical study of WM diffusivity measures in relation to cerebral GM atrophy, damage to most WM tracts as measured in amnestic Mild Cognitive Impairment (MCI) patients did not correlate with estimated GM atrophy, while anatomically congruent relationships between WM measures and GM atrophy was observed in Alzheimer`s disease [28]. The authors of this study concluded that in Alzheimer`s disease, the observed patterns of WM abnormalities may reflect the advanced phase of a secondary degenerative process, and an association, especially in the early phases of the disease, with primary WM tract damage over and beyond GM abnormalities [28]. The same conclusion was drawn in a study by Salat et al. [29], who showed that microstructural WM tissue changes in AD was partly independent of GM degeneration. Furthermore, lower baseline FA has been independently associated with an increased risk of conversion from normal WM to WM hyperintensities, which may suggest a contribution of WM damage to cognitive decline over and above GM

atrophy [30]. In another study, however, where GM volume was found to explain most DTI differences among Alzheimer`s disease patients, amnestic MCI and healthy controls, it was suggested that most DTI-derived changes in AD and amnestic MCI were largely secondary to GM atrophy [31]. Uncertainty remains, but in a recent review of the sparse literature on this topic, it was suggested that microstructural WM affection at pre-Alzheimer`s disease stages cannot be completely accounted for by concomitant GM atrophy [32]. This is further supported by a recent post-mortem study suggesting that WM Aβ peptides accumulate independent of overall grey matter fibrillar amyloid pathology [33]. As noted, even less is known about the relation between GM and WM changes in normal aging. However, due to the intrinsically specific relations of distinct WM tracts and their cortical afferent and efferent projections, and as studies have also pointed to some degree of regional variation in age effects on both cortical and white matter, we believe that some extent of specificity can be tentatively hypothesized.

Based on previous theoretical and empirical accounts, as reviewed above, the following broad hypotheses concerning changes across a 3.6 year period for persons distributed across the adult lifespan (age 20–87 years) were tested:

1. There will be significant age-related increases in mean (MD), radial (RD), and axial (AD) diffusivity along with decreases in fractional anisotropy (FA) for multiple WM tracts.
2. Observed WM changes will be significantly related to cortical changes, with increases in diffusivity and decreases in FA relating to increased cortical thinning. These relationships will show some degree of anatomical specificity, corresponding to areas which the tracts in question connect.

Material and Methods

Sample

The longitudinal sample was drawn from the ongoing project *Cognition and Plasticity through the Lifespan*, run by the Research Group for Lifespan Changes in Brain and Cognition, Department of Psychology, University of Oslo [12, 34]. Written informed consent was obtained from all participants, and all procedures were conducted in compliance with the Code of Ethics of the World Medical Association (Declaration of Helsinki) and were approved by the Regional Committee for Medical and Health Research Ethics (REC South East Norway). For the first wave of data collection, participants were recruited mainly through newspaper ads. Recruitment for the second wave was by written invitation to the original participants. At both time points (Tp1, Tp2), participants were screened with a standardized health interview. This health interview did not involve a formal psychiatric screening, but included questions on current and former treatment for psychiatric and other medical conditions as well as self-disclosure of any medications used. Exclusion criteria were history of injury or disease known to affect central nervous system (CNS) function, including neurological or psychiatric illness or serious head trauma, being under psychiatric treatment, use of psychoactive drugs known to affect CNS functioning, and MRI contraindications. Participants were required to be right handed, fluent Norwegian speakers, and have normal or corrected to normal vision and hearing. Participants were required to score $\geq$26 on the Mini Mental State Examination (MMSE; [35], have a Beck Depression Inventory (BDI); [36] score below the threshold for moderate depression ($\leq$16), and score $\geq$85 on the Wechsler Abbreviated Scale of Intelligence (WASI) [37].

At follow-up an additional set of inclusion criteria was employed: MMSE score $\geq$26; MMSE change from Tp1–Tp2 $<$ 10%; California Verbal Learning Test II–Alternative Version (CVLT II; [38] immediate delay and long delay T-score $>$ 30; CVLT II immediate delay and long delay

change from Tp1-Tp2 < 60%. At both time points all scans were evaluated by a neuroradiologist and were required to be deemed free of injuries or conditions requiring clinical follow-up.

Two hundred and eighty-one participants completed Tp1 assessment. For the follow-up study, 42 opted out, 18 could not be located, 3 did not participate due to health reasons (the nature of these were not disclosed), and 3 had MRI contraindications, yielding a total of 66 dropouts (35 females, mean (SD) age = 47.3 (20.0) years). Independent samples *t*- tests revealed that dropouts had significantly lower FSIQ (t = -3.92, p < 0.001) and BDI (t = -2.02, p = 0.046) scores but comparable CVLT and MMSE scores (p's > .05). More detailed dropout characteristics are published elsewhere (Storsve et al., 2014). Of the 215 participants that completed MRI and neuropsychological testing at both time points, 8 failed to meet one or more of the additional inclusion criteria for the follow-up study described above, 4 did not have adequately processed diffusion MRI data, and two were outliers (four or more tracts showing change values >6 SD from mean). This resulted in a final follow-up sample of 201 participants (118 females) aged 20–84 years at Tp1 and 23–87 years at Tp2. Mean (SD) age was 50.0 (16.5) years at Tp1 and 53.6 (16.5) years at Tp2. Mean (SD) scan interval was 3.6 (0.5) years (range: 2.7–4.8 years). An independent samples t-test revealed no age (t = -1.47, p = 0.15) or scan interval (t = -0.56, p = 0.57) differences between males and females. Sample characteristics are presented in Table 1.

Participants included in analyses performed well above average on cognitive tests and passed a thorough screening procedure including health interview, cognitive assessments and radiological evaluation, thus minimizing the likelihood of current psychological or neurological diagnoses confounding results. However, it should be noted that although our primary focus has been to retain a healthy sample, the high level of functioning generally displayed by our participants means that they cannot be considered representative of the population of adults as a whole. For example, given that general cognitive ability is associated with a thicker cortex [39, 40] and increased WM integrity [41], it is possible that the present results to some extent overestimate absolute thickness and WM integrity values as compared to a more representative sample. It is unclear, however, whether this sample bias towards higher functioning individuals could translate to an underestimation of change estimates, as compared to a more representative sample.

Table 1. Characteristics of participants (n = 201, 118/83 females/males) at the two time points (Tp1 and Tp2).

	Tp1		Tp2		Tp2-Tp1
	Mean	**SD**	**Mean**	**SD**	**Difference**
Age	50.0	(16.5)	53.6	(16.5)	**3.6**
Education	15.9	(2.6)	3.3	(0.7)	*NA*
MMSE	29.4	(0.7)	29.1	(1.0)	**-0.3**
CVLT II IR	56.5	(11.7)	58.1	(11.1)	**1.6**
CVLT II SDR	12.3	(2.9)	12.9	(2.9)	**0.5**
CVLT II DR	12.8	(2.9)	13.1	(2.7)	0.3
FSIQ	115.8	(8.6)	119.1	(9.7)	**3.3**
BDI	4.5	(3.9)	*NA*		*NA*

Tp2-Tp1 represents the observed changes within the sample from Tp1 to Tp2. Age = Age at MR scan; Education = years of education (note: at Tp2 we introduced a categorical classification system on a 4-point scale, with 1 = Primary school (9 years), 2 = High school (12 years), 3 = Bachelor´s degree, 4 = Master´s degree or higher); MMSE = Mini Mental State Examination (max score = 30); CVLT II IR = Total California Verbal Learning Test (Version II) immediate recall (max score = 80); CVLTII SDR = short delay recall (5 minutes) (max score = 16); CVLT II DR = delayed recall (30 minutes) (max score = 16); FSIQ = Full Scale IQ (note: 4-component WASI at Tp1 and 2-component WASI at Tp2).; BDI = Beck Depression Inventory (Tp1 only). For mean difference scores: **Bold** if p < 0.05.

doi:10.1371/journal.pone.0156770.t001

MRI acquisition

Imaging data was collected using a 12- channel head coil on a 1.5 T Siemens Avanto scanner (Siemens Medical Solutions; Erlangen, Germany) at Rikshospitalet, Oslo University Hospital. The same scanner and sequences were used at both time-points. Data for morphometric analyses were acquired with two repetitions of a sagittal T_1-weighted magnetization prepared rapid gradient echo (MPRAGE) sequence per participant per visit, with the following parameters: repetition time/echo time /time to inversion/flip angle = 2400 ms/3.61 ms/1000 ms/8°, matrix = 192 × 192, field of view = 240, 160 slices voxel size = 1.25 × 1.25 × 1.20 mm. Scanning time for each MPRAGE sequence was 7 min 42 s.

The pulse sequence used for diffusion weighted imaging was a single-shot twice-refocused spin-echo echo planar imaging (EPI) with 30 directions with the following parameters: repetition time (TR)/echo time (TE) = 8200 ms/82 ms, b-value = 700 s/mm^2, voxel size = 2.0 × 2.0 × 2.0 mm, field of view = 256, matrix size = 128 × 128 × 64, primary slice direction = axial, phase encoding direction = columns. This sequence is designed to minimize eddy current-induced image distortions [42]. The sequence was repeated in two successive runs, each including 10 non diffusion-weighted (b = 0) images and 30 diffusion weighted images. Total scanning time was 11 min 21 s.

MRI analysis

Morphometric analyses. The raw data were reviewed for quality, and automatically corrected for spatial distortion due to gradient nonlinearity [43] and B_1 field inhomogeneity [44]. For all participants, the two image volumes collected at each time point were co-registered, averaged to improve the signal-to-noise ratio (SNR), and resampled to isotropic 1-mm voxels. Images were first automatically processed cross-sectionally (independently) for each time point with the FreeSurfer software package (version 5.1.0; Athinoula A. Martinos Center for Biomedical Imaging, Boston, MA), which is documented and freely available online (http://surfer.nmr.mgh.harvard.edu/). This processing includes motion correction, removal of non-brain tissue, automated Talairach transformation, intensity correction, volumetric segmentation [45], and cortical surface reconstruction [46–48] and parcellation [49, 50]. All volumes were inspected for accuracy and minor manual edits were performed where needed by a trained operator, usually restricted to removal of nonbrain tissue included within the cortical boundary. To extract reliable longitudinal cortical volume, thickness and area change estimates, the cross-sectionally processed images were subsequently run through the longitudinal stream in FreeSurfer [51]. Here, an unbiased within-subject template volume based on the two cross-sectional images is created for each participant, and processing of both time points are then initialized using common information from this template. This increases sensitivity and robustness of the longitudinal analysis [51]. The registration method used to generate the within-subject template from Tp1 and Tp2 ensures inverse consistency [52], meaning that the transform computed from Tp2 to Tp1 is the inverse of that computed from Tp1 to Tp2 [53], which is critical in longitudinal analyses [54]. In addition, new probabilistic methods (temporal fusion) were applied to further reduce the variability across time points. Surface maps were resampled, mapped to a common surface, smoothed using a circularly symmetric Gaussian kernel with a full-width half-maximum of 15 mm [55] and submitted to statistical analyses.

Diffusion weighted MRI analyses. All diffusion weighted (DW) images and tractography reconstructions were manually checked and scans with major artefacts were excluded. For each DW-MRI scan, we aligned all images in the series to the first non-diffusion-weighted image using affine registration [56] to reduce misalignment between the images due to head motion and eddy currents, and we reoriented the corresponding diffusion-weighting gradient vectors accordingly [57, 58].

Within each time point, the subject's non-diffusion-weighted (b = 0) images and T_1-weighted images were aligned with boundary-based registration [59]. This is a method for within-subject, cross-modal registration that optimizes the contrast of the b = 0 images across the grey/white matter surface obtained from the T_1-weighted images.

We used a longitudinal extension to the TRActs Constrained by UnderLying Anatomy (TRACULA) in FreeSurfer (version 5.3.0) to delineate 18 major WM fascicles in each participant`s DW-MRI data [21, 22]. TRACULA is an algorithm for automated global probabilistic tractography that estimates the posterior probability of each of the 18 pathways given the DW-MRI data [21, 22]. The posterior probability is decomposed into a data likelihood term, which uses the "ball-and-stick" model of diffusion [60], and a pathway prior term, which incorporates prior anatomical knowledge on the pathways from a set of training subjects. The information extracted from the training subjects is the probability of each pathway passing through (or next to) each anatomical segmentation label. This probability is calculated separately for every point along the trajectory of the pathway. Thus there is no assumption that the pathways have the same shape in the study subjects and training subjects, only that the pathways traverse the same regions relative to the surrounding anatomy. In other words, TRACULA does not rely on perfect alignment between the study subjects and training subjects. The anatomical segmentation labels required by TRACULA were obtained by processing the T_1-weighted images of the study subjects with the automated cortical parcellation and subcortical segmentation tools in FreeSurfer (see previous section). In the longitudinal version of TRACULA, the joint posterior probability of the pathway given the DW-MRI data and anatomical segmentations of *all* time points is computed. This has been shown to improve both test-retest reliability and sensitivity to longitudinal WM changes, when compared to reconstructing the pathways at each time point independently [22].

The pathways reconstructed by TRACULA are displayed in Fig 1: corticospinal tract (CST), uncinate fasciculus (UNC), inferior longitudinal fasciculus (ILF), anterior thalamic radiations

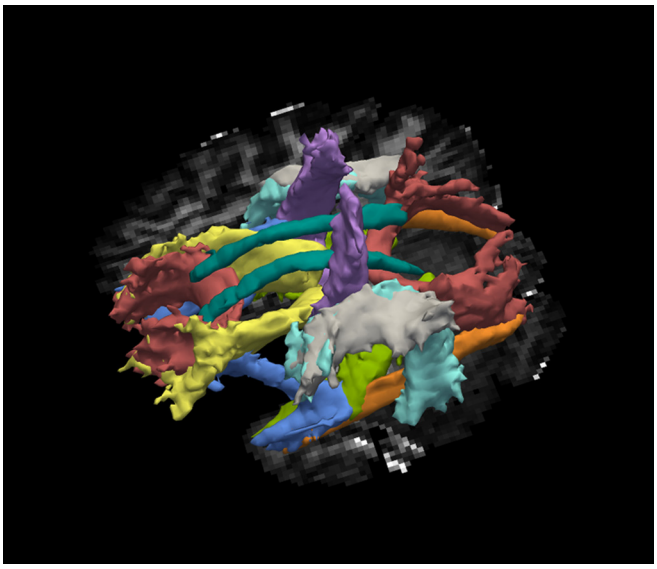

Fig 1. All tracts as delineated by TRACULA. Red = Forceps Major (posterior)/Forceps Minor (anterior), Yellow = Anterior Thalamic Radiation, Light green = Cingulum Angular Bundle, Dark green = Cingulum Cingular Bundle, Purple = Corticospinal Tract, Orange = Inferior Longitudinal Fasciculus, Gray = Superior Longitudinal Fasciculus Parietal part, Aquamarine = Superior Longitudinal Fasciculus Temporal part, Blue = Uncinate Fasciculus.

doi:10.1371/journal.pone.0156770.g001

(ATR), cingulum–cingulate gyrus bundle (CCG), cingulum–angular bundle (CAB), superior longitudinal fasciculus-parietal terminations (SLFP), superior longitudinal fasciculus-temporal terminations (SLFT), corpus callosum–forceps major (FMaj), and corpus callosum–forceps minor (FMin). Other than the corpus callosum, all pathways are reconstructed for the left (L) and right (R) hemisphere.

We obtained mean values of the FA, MD, RD, and AD in each of the 18 WM pathways reconstructed by TRACULA for each participant and each time point. To compute these mean values, the pathway distributions were thresholded at 20% of their maximum value, and the FA, MD, RD, and AD values at each voxel were weighted by the pathway probability at that voxel. We also computed the average FA, MD, RD, and AD in the entire WM for each subject. For this purpose we generated a WM mask from the subject's anatomical segmentation and mapped it from the space of the T1-weighted image to the space of the DWIs. Note that the tensor model was fit to the data only to extract these anisotropy and diffusivity measures, and not to perform the tractography in TRACULA, which relies on the ball-and-stick model of diffusion instead.

Head motion. As head motion has previously been shown to produce spurious findings in DW-MRI studies [61], care was taken to control for head motion in the present study. To quantify head motion in each scan, we derived volume-by-volume translation and rotation from the affine registration, as well as slice-by-slice signal drop-out measures that are specific to DW-MRI [62]. The registration-based measures are better at capturing slower, between-volume motion, whereas the intensity-based measures are better at capturing more rapid, within-volume motion. A total motion index (TMI) at each time point was computed from these measures, as described in, and included as covariates in subsequent analyses

Tract endings. To visualize the endings of the WM pathways on the cortical surface, we mapped the probability distribution of each of the two endings of each pathway, as computed by TRACULA, from its native DW-MRI space to the space of the corresponding T_1-weighted images. We projected the end points onto the grey/white matter surface by sampling along the surface normal vector, anywhere within 4mm (2 DWI-space voxels) of the gray/white junction, and then smoothing along the surface with a 2D Gaussian kernel of 2mm full width at half max. We transformed the resulting surface maps to the fsaverage template (included in FreeSurfer) and averaged them across all subjects and time points. The vertices with the top 25% values were retained from each average map to create a label of the average tract endings, for comparison with subsequent group analyses of cortical thickness.

Statistical analyses

Statistical analyses were performed by use of FreeSurfer 5.3.0 and IBM SPSS Statistics 20.0. Longitudinal change in cortical thickness and FA, RD, AD, and MD in each hemisphere was calculated as annual percentage change per year (APC; i.e., the annual rate of change with respect to tp1).

One sample t-tests were first used to test whether longitudinal change was significantly different from zero for each of the 18 Tracts of Interest (TOIs). GLMs testing the effects of Tract, Hemisphere, and Sex on FA, AD, RD and MD changes were then carried out in SPSS. Average WM changes across all tracts were also calculated, and we tested which of the diffusion metrics that changed the most. Pearson correlations between age and change were then calculated for all diffusion measures in each TOI, and Fischer r-to-z transformations were used to compare age–diffusion change correlation coefficients between hemispheres. All TOI results were Bonferroni-corrected by a factor corresponding to the number of TOIs, i.e. 18 for one-sample tests, roughly corresponding to a corrected alpha of 0.003, and 8 (one for each bilateral tract) for

analysis comparing the left and right hemisphere, roughly corresponding to a corrected alpha of 0.006.

A series of general linear models (GLMs), as implemented in Freesurfer, were used to perform vertex-wise cortical analyses of the relationship between APC in cortical thickness (dependent variable) and MD and FA in each of the 18 tracts (entered as independent variables in separate analyses). Corrections for multiple comparisons were ensured by testing results against an empirical null distribution of maximum cluster size across 10,000 iterations using Z Monte Carlo simulations as implemented in FreeSurfer [63, 64], synthesized with a cluster-forming threshold of $p < 0.05$ (two-sided). In each of these analyses, sex, age, age squared, scan interval (time elapsed between tp1 and tp2 MRI sessions) and an index for head motion during MR scanning (TMI) at each time point were included as covariates. Results from these GLMs were displayed on a semi-inflated template brain.

Results

Table 2 shows mean Annual Percentage Change (APC) in MD, AD, RD, and FA for each tract. Significant increases in MD, RD, and AD were found for all tracts except right hemisphere CAB and ILF. Significant decreases in FA were evident in all tracts except FMaj, Fmin, left hemisphere CAB, ILF and SLFT, as well as right hemisphere CST. Across tracts, the greatest magnitude of change was apparent for RD (average APC = 0.60), followed by MD (average APC = 0.43), AD (average APC = 0.29) and FA (average APC = -0.27). Correlations between

Table 2. Mean Annual Percentage Change (APC) for the tracts.

		MD			AD			RD			FA		
Tract	**Hemi**	**APC**	**SD**	***p***	**APC**	**SD**	***p***	**APC**	**SD**	***p***	**APC**	**SD**	***p***
FMaj		0.63	1.07	**<0.001**	0.57	0.82	**<0.001**	0.73	1.62	**<0.001**	-0.01	0.81	0.81
FMin		0.26	0.93	**<0.001**	0.19	0.76	**0.001**	0.36	1.47	**0.001**	-0.15	1.09	*0.05*
ATR	rh	0.58	0.78	**<0.001**	0.10	0.69	*0.04*	1.08	1.16	**<0.001**	-1.05	1.14	**<0.001**
ATR	lh	0.49	1.03	**<0.001**	0.19	0.78	**0.001**	0.81	1.42	**<0.001**	-0.66	1.11	**<0.001**
CAB	rh	-0.14	2.69	0.46	0.09	1.93	0.51	-0.33	4.01	0.25	0.89	3.96	**0.002**
CAB	lh	0.32	1.48	**0.002**	0.29	1.36	**0.003**	0.38	1.92	*0.005*	-0.01	1.95	0.95
CCG	rh	0.75	1.41	**<0.001**	0.42	1.19	**<0.001**	1.19	2.45	**<0.001**	-0.43	1.58	**0.005**
CCG	lh	0.44	1.33	**<0.001**	0.14	1.16	0.10	0.89	2.36	**<0.001**	-0.53	2.02	**<0.001**
CST	rh	0.56	1.59	**<0.001**	0.35	1.04	**<0.001**	0.83	2.43	**<0.001**	-0.28	1.37	**0.005**
CST	lh	0.53	1.04	**<0.001**	0.36	0.78	**<0.001**	0.76	1.64	**<0.001**	-0.25	0.96	**<0.001**
ILF	rh	-0.17	1.41	0.09	0.03	0.92	0.69	-0.37	2.30	*0.02*	-0.46	1.94	**0.001**
ILF	lh	0.27	0.89	**<0.001**	0.35	0.84	**<0.001**	0.19	1.19	*0.03*	0.15	0.99	*0.03*
SLFP	rh	0.92	1.45	**<0.001**	0.66	0.99	**<0.001**	1.19	2.01	**<0.001**	-0.51	1.54	**<0.001**
SLFP	lh	0.54	0.98	**<0.001**	0.44	0.78	**<0.001**	0.66	1.33	**<0.001**	-0.28	1.09	**<0.001**
SLFT	rh	0.65	1.27	**<0.001**	0.37	0.87	**<0.001**	0.96	1.82	**<0.001**	-0.53	1.42	**<0.001**
SLFT	lh	0.38	0.77	**<0.001**	0.34	0.63	**<0.001**	0.44	1.08	**<0.001**	-0.10	0.88	0.13
UNC	rh	0.30	0.92	**<0.001**	0.14	0.71	*0.007*	0.48	1.32	**<0.001**	-0.37	1.24	**<0.001**
UNC	lh	0.40	1.37	**<0.001**	0.23	1.01	**0.001**	0.58	1.85	**<0.001**	-0.32	1.26	**<0.001**

Depicted are mean annual percentage change (APC) of mean (MD), axial (AD), and radial (RD) diffusivity and fractional anisotropy (FA) for each tract across the scan interval. FMaj = Forceps Major, FMin = Forceps Minor, ATR = Anterior Thalamic Radiation, CAB = Cingulum Angular Bundle, CCG = Cingulum Cingular Bundle, CST = Corticospinal Tract, ILF = Inferior Longitudinal Fasciculus, SLFP = Superior Longitudinal Fasciculus Parietal part, SLFT = Superior Longitudinal Fasciculus Temporal part, UNC = Uncinate Fasciculus. Bonferroni-corrected at factor of 18, p values are significant p = 0.003.

doi:10.1371/journal.pone.0156770.t002

diffusivity change measures were high, with a mean MD change–RD change correlation of 0.94 across all tracts. GLMs revealed significant effects of Tract (MD: $F_{7,70} = 6.6$, $p < 0.001$; AD: $F_{7,70} = 3.7$, $p = 0.002$; RD: $F_{7,70} = 9.0$, $p < 0.001$; FA: $F_{7,70} = 20.9$, $p < 0.001$), suggesting that different tracts show different rates of change for all four diffusion parameters. Table 2 shows that the rank order of change magnitude between tracts was relatively stable across MD, AD, RD and FA (with a noticeable exception found for FMaj, which showed no change in FA but high levels of change on MD, RD, and AD). Across all measures (diffusion indices and hemisphere), most absolute change was observed for SLFP (APC = 0.65), ATR (APC = 0.62), CCG (APC = 0.60), CST (APC = 0.49), FMaj (APC = 0.49) and SLFT (APC = 0.47), whereas ILF (APC = 0.20), FMin (APC = 0.24), CAB (APC = 0.30), and UNC (APC = 0.35) showed less change. Furthermore, GLMs did not reveal any significant main effects of Sex and Hemisphere on changes in MD, AD, RD, and FA. However, significant Tract × Hemisphere interactions (MD: $F_{7,70} = 18.4$, $p < 0.001$; AD: $F_{7,70} = 7.8$, $p < 0.001$; RD: $F_{7,70} = 16.2$, $p < 0.001$; FA: $F_{7,70} = 10.4$, $p < 0.001$) suggest different patterns of hemispheric differences for different tracts. In general, more absolute change was observed in the right hemisphere (APC = 0.54) than in the left hemisphere (APC = 0.40), but this varied with tract. Post hoc tests revealed significantly greater APC in the right hemisphere for ATR (RD, FA: $p < 0.001$), CAB (FA: $p < 0.001$), CCG (AD: $p = 0.001$; MD: $p < 0.001$) and SLFT (RD, FA: $p < 0.001$), and significantly greater APC in the left hemisphere for ILF (AD: $p < 0.001$).

Table 3 displays Pearson correlations between changes in APC in the four measures (MD, AD, RD, FA) and age. In general, positive correlations with age were found for MD, AD, and

Table 3. Pearson correlations between annual percent change (APC) and age.

		MD		AD		RD		FA	
Tract	**Hemi**	r_{Age}	*p*	r_{Age}	*p*	r_{Age}	*p*	r_{Age}	*p*
FMaj		0.35	**<0.001**	0.36	**<0.001**	0.29	**<0.001**	-0.08	0.26
FMin		0.40	**<0.001**	0.44	**<0.001**	0.29	**<0.001**	-0.08	0.28
ATR	rh	0.45	**<0.001**	0.36	**<0.001**	0.40	**<0.001**	-0.24	**0.001**
ATR	lh	0.53	**<0.001**	0.50	**<0.001**	0.49	**<0.001**	-0.32	**<0.001**
CAB	rh	-0.03	0.65	-0.05	0.52	-0.02	0.74	0.01	0.91
CAB	lh	0.13	0.06	0.06	0.42	0.16	*0.02*	-0.12	0.10
CCG	rh	0.26	**<0.001**	0.07	0.36	0.29	**<0.001**	-0.26	**<0.001**
CCG	lh	0.33	**<0.001**	0.14	*0.05*	0.34	**<0.001**	-0.28	**<0.001**
CST	rh	0.18	*0.01*	0.24	**<0.001**	0.14	*0.05*	-0.04	0.57
CST	lh	0.36	**<0.001**	0.44	**<0.001**	0.26	**<0.001**	-0.08	0.25
ILF	rh	0.01	0.92	-0.02	0.75	0.02	0.83	-0.03	0.72
ILF	lh	0.29	**<0.001**	0.19	*0.01*	0.31	**<0.001**	-0.17	*0.02*
SLFP	rh	0.24	**<0.001**	0.21	*0.004*	0.24	**0.001**	-0.23	**0.001**
SLFP	lh	0.41	**<0.001**	0.39	**<0.001**	0.38	**<0.001**	-0.22	**0.001**
SLFT	rh	0.23	**0.001**	0.23	**0.001**	0.21	**0.003**	-0.16	*0.02*
SLFT	lh	0.44	**<0.001**	0.43	**<0.001**	0.38	**<0.001**	-0.16	*0.03*
UNC	rh	0.14	*0.05*	0.16	*0.02*	0.11	0.13	-0.001	0.99
UNC	lh	0.20	*0.01*	0.19	*0.01*	0.19	*0.01*	-0.14	*0.04*

Mean (MD), axial (AD), and radial (RD) diffusivity and fractional anisotropy (FA) for each tract. FMaj = Forceps Major, FMin = Forceps Minor, ATR = Anterior Thalamic Radiation, CAB = Cingulum Angular Bundle, CCG = Cingulum Cingular Bundle, CST = Corticospinal Tract, ILF = Inferior Longitudinal Fasciculus, SLFP = Superior Longitudinal Fasciculus Parietal part, SLFT = Superior Longitudinal Fasciculus Temporal part, UNC = Uncinate Fasciculus. Bonferroni-corrected at factor of 18, p values are significant p = 0.003.

doi:10.1371/journal.pone.0156770.t003

RD, indicating that older adults showed relatively greater increases in these measures, and negative correlations with age were found for FA, suggesting a greater decrease in FA with advancing age. Significant age correlations were most frequent for MD, AD, and RD, with FA only being significantly related to age for ATR, CCG and SLFP. FMaj and FMin displayed significant correlations with age for MD, AD, and RD ($ps < 0.001$), but showed no such relationship for FA (r = -0.08 for both, lowest p = 0.26). CAB and UNC were the only tracts not showing any significant change relationships with age. Only one significant hemisphere difference in age correlations was detected by Fischer r-to-z transformations (ILF MD: z = 2.87, $p = 0.004$).

Tracts showing significant change were selected for further testing of cortical thickness change–white matter integrity change relationships. Monte Carlo simulations revealed several clusters of significant relationships between diffusivity changes in these selected tracts and changes in cortical thickness. Figs 2 and 3 display significant MD change–thickness change relationships, and reveals an overall pattern of negative correlations (due to the high correlation between diffusivity change measures, RD change–thickness change and AD change–thickness change are not displayed). That is, greater reductions in cortical thickness were generally associated with greater increases in MD. Fig 4 reveals a predominantly opposite pattern between thickness change and FA change, with less thinning generally being associated with a greater increase in FA. A more detailed description of the effects shown in Figs 2 and 4 is given in S1 File. Overall, effects appeared mixed with regard to regions overlapping with projected tract endings and in areas not confined to these.

Discussion

In the present study, widespread microstructural WM tract changes were observed in healthy adults across a period of 3.6 years. For most tracts, these changes were related to cortical changes both globally and with some degree of tract endpoint specificity, thus demonstrating a relationship between WM tract and cortical GM changes. The extent to which each of the specific hypotheses was supported is discussed below.

Hypothesis 1: There will be significant age-related increases in MD, RD, and AD along with decreases in FA for multiple white matter tracts

The hypothesized age-related increases in MD, RD, and AD and decreases in FA were observed for multiple WM tracts. Across all tracts, the greatest changes were observed for RD (average APC = 0.68), followed by MD (average APC = 0.43), AD (average APC = 0.35), and FA (average APC = -0.27). This pattern of greater change in RD than AD with increasing age has been reported previously [65], and is thought to reflect that WM integrity reductions in aging is a primarily a consequence of a loss in myelin integrity (reflected by increases in RD) rather than changes in axonal size or axonal injury (reflected by increases in AD) [65, 66]. Furthermore, less overall change in FA than in MD and RD has previously been reported in a longitudinal study across a 2-year interval [67] as well as cross-sectionally [68], and the observed pattern of positive (MD, RD, AD) and negative (FA) changes with age is consistent with previous cross-sectional studies showing age-related decline in white matter integrity [15, 69–71]. The present longitudinal study provides strong evidence for a general age-dependent deterioration of tract WM integrity across the adult lifespan, and provides detailed information on changes in a high number of tracts.

Significant changes were found for most tracts, with the exception of right hemisphere cingulum–angular bundle and inferior longitudinal fasciculus, as well as in forceps major and forceps minor FA. Patterns of changes were relatively similar across AD, RD and MD, with relatively pronounced changes observed for superior longitudinal fasciculus-parietal

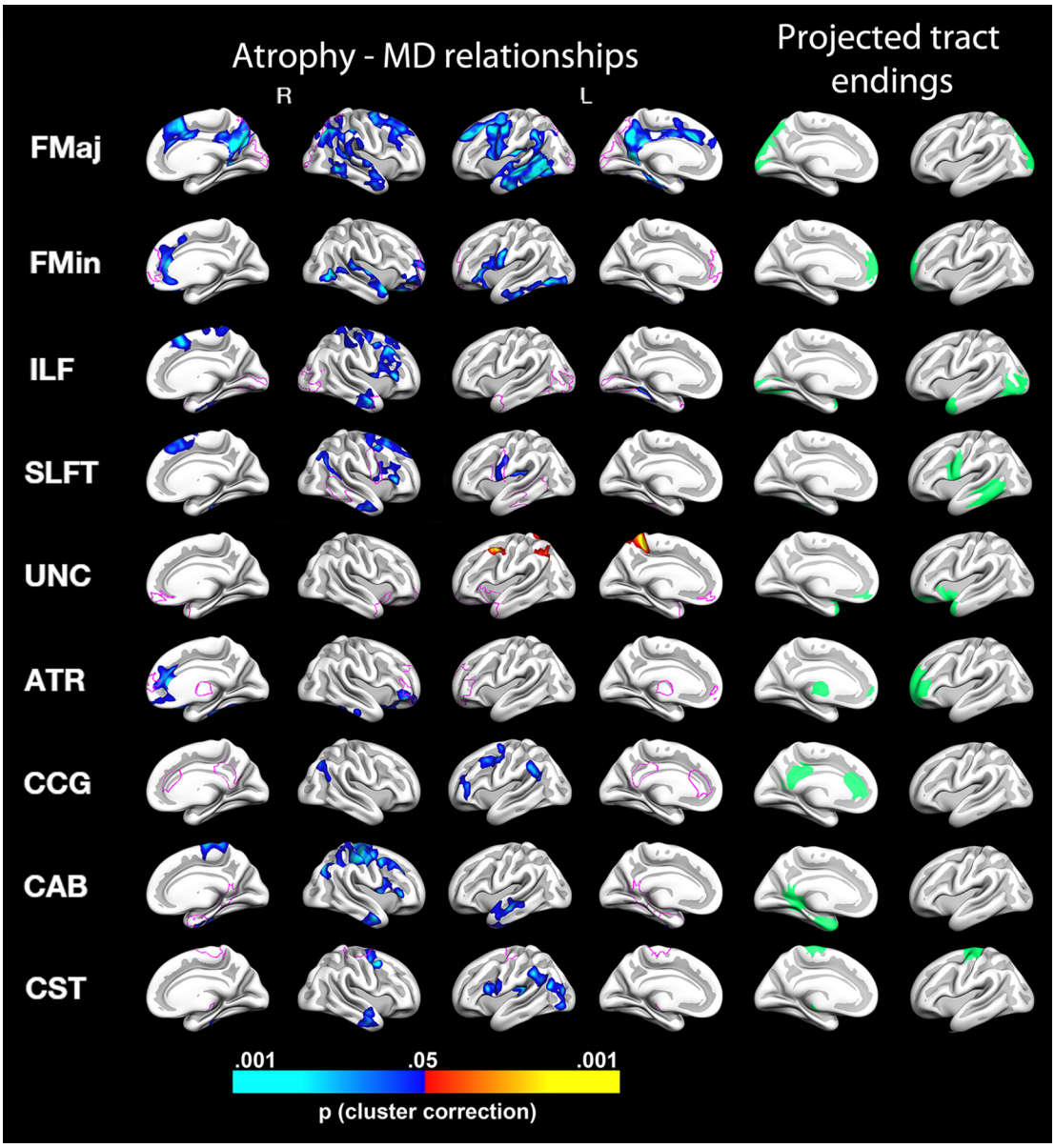

Fig 2. Relationships between changes in mean diffusivity (MD) and changes in cortical thickness. The figure depicts, from the left to right: relationships for the medial and lateral view of the right hemisphere, the lateral and medial view of the left hemisphere, and the cortical areas where the tracts project are shown for the left hemisphere in medial and lateral view, respectively. Blue color denotes significant negative relationships, i.e. more cortical thinning with greater increases in MD, and red color denote positive relationships (i.e. relatively less cortical thinning with greater increases in MD). Pink lines displayed on the cortical surface represent an outline of the estimated tract endings. FMaj = Forceps Major, FMin = Forceps Minor, ILF = Inferior Longitudinal Fasciculus, SLFT = Superior Longitudinal Fasciculus Temporal part, UNC = Uncinate Fasciculus ATR = Anterior Thalamic Radiation, CCG = Cingulum Cingular Bundle, CAB = Cingulum Angular Bundle, CST = Corticospinal Tract. For all significant tract relationships except for that of the uncinate, increasing MD related to increased cortical thinning in select areas.

doi:10.1371/journal.pone.0156770.g002

terminations, anterior thalamic radiations, the cingulum–cingulate gyrus bundle, corticospinal tract, forceps major, and superior longitudinal fasciculus-temporal terminations, with more moderate changes being found in inferior longitudinal fasciculus, forceps minor, cingulum–angular bundle, and uncinate fasciculus. These findings are in line with previous cross-sectional reports as well as our own longitudinal voxel-based investigation showing that superior

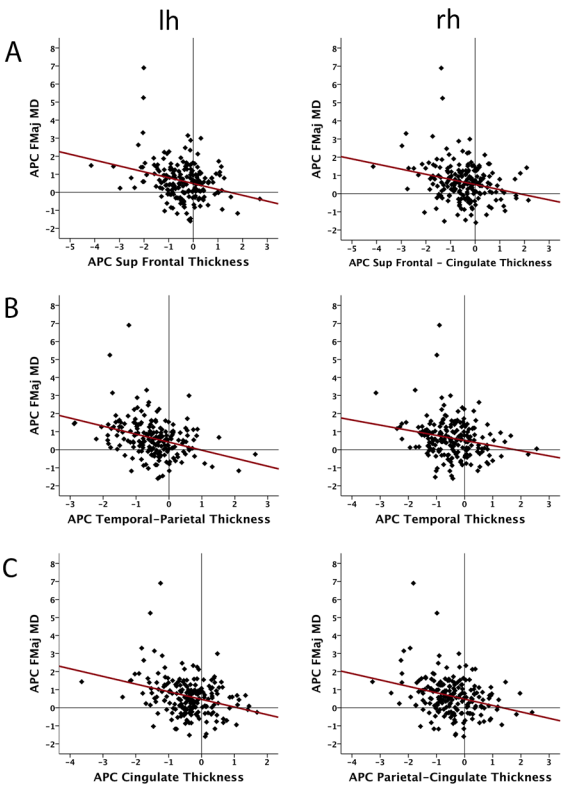

Fig 3. Scatterplots depicting the relationship between annual percent change (APC) in mean diffusivity (MD) of the forceps major (Fmaj) and cortical thickness change. The select areas shown are those showing significant relationships depicted in the upper panel of Fig 2. Panel A depicts relationships in left hemisphere (lh) superior frontal (sup front) and right hemisphere (rh) superior frontal and cingulate cortices, Panel B depicts relationship in left temporal parietal and right temporal cortices, and panel C depicts relationships in the left cingulate and right parietal and cingulate cortices.

doi:10.1371/journal.pone.0156770.g003

WM tracts display more rapid degeneration than inferior tracts [13, 68, 72]; tracts with superior tract endings, such as superior longitudinal fasciculi and the corticospinal tract all change to a greater extent than do tracts with more inferior tract endings, such as longitudinal fasciculus, cingulum–angular bundle, and uncinate fasciculus. Furthermore, although high levels of age-related decrease were observed in anterior thalamic radiations, we found relatively high levels of change also in forceps major and relatively low levels of change in forceps minor. Thus, our findings at the level of specific tracts also fit better with the notion that an inferior to superior gradient is more predominant than that of a posterior to anterior gradient of vulnerability, as previously observed with voxel-based methods [13]. Interestingly, an inferior to superior gradient of WM maturation has previously been reported in a cross-sectional study in adolescents [73]. This could indicate that late developing WM tracts show increased overall deterioration across adulthood. Indeed, superior longitudinal fasciculi and corticospinal tract APC showed relatively high correlations with age compared to most other tracts, indicating that these tracts are particularly vulnerable to the effects of aging, which may be consistent with a "last-in-first-out" hypothesis of lifespan WM development [74]. At present this interpretation remains uncertain, however, and further studies covering the entire human lifespan are needed to test this notion.

Furthermore, several hemispheric differences were found with the right hemisphere showing greater change for anterior thalamic radiations, cingulum–angular bundle, cingulum–cingulate

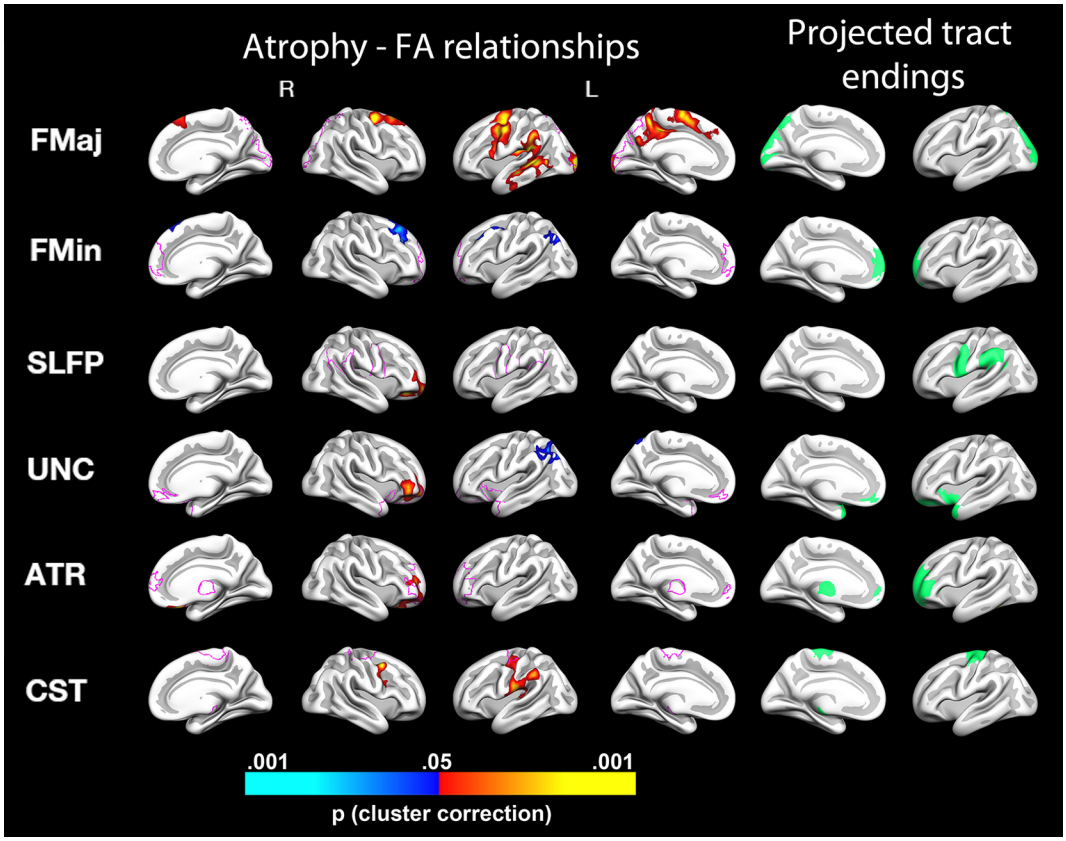

Fig 4. Relationships between changes in fractional anisotropy (FA) and changes in cortical thickness. The figure depicts, from the left to right: relationships for the medial and lateral view of the right hemisphere, the lateral and medial view of the left hemisphere, and the cortical areas where the tracts project are shown for the left hemisphere in medial and lateral view, respectively. Red color denotes significant positive relationships, i.e. more cortical thinning with greater decreases in FA, and blue color denote negative relationships (i.e. more cortical thinning with lesser decrease in FA). Pink lines displayed on the cortical surface represent an outline of the estimated tract endings. FMaj = Forceps Major, FMin = Forceps Minor, SLFP = Superior Longitudinal Fasciculus Parietal part, UNC = Uncinate Fasciculus, ATR = Anterior Thalamic Radiation, CST = Corticospinal Tract. As can be seen, for all tracts except for the Forceps Minor, decreasing FA related to cortical thinning in select areas, and for the Uncinate fasciculus, a mixed relationship across areas was seen.

doi:10.1371/journal.pone.0156770.g004

gyrus bundle, inferior longitudinal fasciculus, and superior longitudinal fasciculus-temporal terminations. Hemispheric asymmetry in the strength of white matter pathways have previously been reported in temporoparietal junction-insula and temporoparietal junction-frontal connections [75], but we are not aware of other studies showing age-dependent changes in specific tracts to be hemisphere-dependent in adulthood.

Hypothesis 2: Observed white matter changes will be significantly related to cortical changes, with increases in diffusivity and decreases FA relating to increased cortical thinning, and these relationships will show some degree of anatomical specificity, corresponding to areas which the tracts in question connect

As hypothesized, several relationships between changes in cortical thickness and changes in WM integrity of specific tracts were found. These relationships were almost exclusively in the hypothesized direction, with cortical thinning related to increases in MD and decreases in FA.

In general, the present findings are thus consistent with mechanical theories that posit a causal relationship between changes in white matter and cortical structure. In line with Wallerian degeneration, it is possible that cortical thinning precedes and causes WM deterioration through neural death and subsequent degeneration of the axon and myelin sheets [1, 2]. Indeed, it has been suggested that DTI-derived changes in Alzheimer`s disease and amnestic MCI may largely be secondary to GM atrophy [31]. However, neuronal death is unlikely as the primary cause of cortical thinning in normal aging, as the amount of cell death in normal aging is limited [76, 77]. One more probable neurobiological cause of cortical thinning is related to reduced number of synapses [78], with accompanying lower metabolic cell activity and shrinkage of the soma [79]. It is conceivable that these changes in turn may affect connecting WM tracts.

It is also possible that the direction of causality for the observed GM-WM relationships is opposite–decreases in axonal or myelin integrity would in and of themselves lead to degeneration of the cortical areas these tracts project to and from [32]. In Alzheimer's Disease, evidence from molecular neurobiology and from human *in vivo* neuroimaging studies indicate that WM abnormalities can precede GM changes, especially in the early phases of the disease, with primary WM tract damage over and beyond GM abnormalities [28] [33]. It may be that similar processes, although of lesser magnitude and severity, can be at play in normal aging. This opens the possibility that changes in WM microstructure potentially can be independent of GM changes, yet contribute to induce GM degeneration. The mechanisms for this in normal lifespan and aging changes are not known, however. One study found caspase-6 activity in the entorhinal cortex and hippocampus in normal aging to be related to cognitive function [80]. Caspase-6 is a protease that induces axonal degeneration, and cleaves Tau and other proteins that are important for cytoskeletal stabilization and thus axonal survival. Such events on the microbiological level may impact axons directly even in GM, thus contributing to create GM-WM relationships as observed in the present study.

We cannot say based on these findings which come first–the cortical thinning, or the WM tract changes. In both cases, however, and for either account to be supported, we would in principle need to see relations to some extent specific to the cortical areas of projection. If a direct causal relationship between WM and GM changes is to be postulated, instead of relationships being caused by general changes in the brain simultaneously ongoing in both WM and in the cortex, we would expect cortical thinning in the regions where a specific tract starts and ends to be more closely related to the integrity changes in that particular tract. To what extent can we say that this is the case in the present data?

There is some evidence of specificity in the present findings. For instance, as seen in Fig 2, increases in MD of the forceps minor relate to cortical thinning of the medial and anteriormost parts of the right prefrontal cortices, in relatively good correspondence with its projected tract endings. The same is true for MD changes of the temporal part of the superior longitudinal fasciculus (SLFT)–relations to cortical change are indeed seen in temporal areas overlapping or in close proximity to the projected tract endings bilaterally. Whereas the corticospinal tract MD and FA cortical change relationships are also seen in slightly more inferior areas, they extend to, or are also found, in overlapping and adjacent areas of the projected corticospinal tract endings, in superior sensorimotor areas. However, there were clearly also relationships of WM tract–cortical change relationships non-specific to the projected tract endpoints. The most widespread effects were seen for forceps major, which connects the occipital lobes, and hence for which we might expect WM change relationships in the occipital cortices. However, this was only partially the case. MD changes of the forceps major were related to thickness changes in clusters including temporal and parietal lobes, as well as parts of the precuneus, retrosplenial cortex, and posterior cingulate cortex. For FA of the forceps major, positive change

relationships with cortical thickness were found in left hemisphere superior temporal, retrosplenial, and precuneus cortices, as well as bilaterally in the superior frontal cortex. The same relative non-specificity of effects is true of many of the areas where relations were identified for WM diffusion and cortical changes. For instance, changes in MD of the inferior longitudinal fasciculus, cingulum (both cingular gyrus and angular bundle) and MD and FA of the corticospinal tract show relations to lateral cortical changes, whereas none of these tracts are estimated to project to lateral endpoints.

Of course, the specific areas of projected tract endings for all tracts are themselves heavily interconnected with other areas. For instance, the occipital areas of forceps major projections are interconnected with e.g. temporal, parietal and frontal cortical areas [81, 82], including in part the areas of effects seen here. Hence, a non-specificity of WM diffusivity and cortical changes cannot be taken as direct evidence against Wallerian degeneration or primary cortical degeneration leading to WM changes across the lifespan in healthy adults. However, the relatively widespread effects may speak of if not global, at least not highly and exclusively specific influences at play.

Some relations of WM and cortical changes opposite of the hypothesized directions were also observed. While we in general found greater increases in MD and decreases in FA to be related to more cortical thinning, there were a few notable exceptions. A mixed relationship was observed for the uncinate fasciculus. A positive thickness change–uncinate MD change as well as a negative thickness change–uncinate FA change cluster was observed laterally in left hemisphere superior parietal cortex, and a positive thickness change–FA change cluster was found laterally in the right hemisphere orbitofrontal cortex. The same was true for forceps minor, where a negative FA-cortical thickness change relationship was observed bilaterally in the caudal middle frontal cortex, as well as in right hemisphere inferior parietal cortex. The neurobiological foundations of such relationships, as well as to what extent they can be consistently observed, remain unknown.

The present findings must be seen in the context of adult lifespan changes, and the underlying mechanisms of the observed relations must hence be complex. While we in the context of age changes in the adult lifespan hypothesized primarily increases in diffusivity and decreases in FA relating to cortical thinning, there may likely be parts of the age range covered where this may not be the case across tracts. As noted, differing lifespan trajectories have been reported for cortical and WM macro-and microstructure [13–18], so that a simple mechanistic relationship between these metrics is unlikely. It may be that differing relationships between cortical thickness and WM tract characteristics can be observed at different ages. Indeed, cross-sectional investigations have yielded differing findings. Negative associations between tract-specific FA and cortical thickness have been reported in younger healthy adults, along with the absence of such associations in schizophrenia [83]. However, another cross-sectional study of healthy young adults found topographical positive associations between FA of the arcuate fasciculus and cortical thickness [84]. Corresponding areas of lower FA in normally appearing WM and regionally lower GM density has been reported in cross-sectional investigation of multiple sclerosis (MS) patients [85], and as mentioned, in amnestic mild cognitive impairment [28]. It is uncertain how such cross-sectional findings relate to longitudinal changes.

Limitations of the present study include a relatively select sample with overall functioning in the superior range. One may thus speculate whether the observed changes and relations may be an underestimation of those existing in the broader population across the adult age range. Despite overall good cognitive function and health, we can still not completely rule out influence of preclinical conditions in the present sample. Future investigations should serve to delineate various influences impacting relationships of white matter tract and cortical change,

including potential lifestyle [86–88] and genetic factors [89, 90]. This may hopefully serve to further delineate specific and global factors at work and their relative impact. Furthermore, alternative statistical approaches, such as for example latent change score modelling, have been shown to be a powerful tool for understanding the directionality of WM-cognition relations in longitudinal samples [91]. Applying these types of advanced statistical methods to voxel-based neurostructural data therefore represents another rich avenue for future research on the relationship between WM and GM changes in adulthood.

Conclusion

The present study points to widespread longitudinal changes in WM microstructure across tracts and metrics that were increasing with age. WM microstructural changes were related to cortical changes in multiple areas, in part overlapping with and in part not confined to the regions of projected tract endings. The present study hence demonstrates that changes in WM microstructure and cortical thickness are related in healthy adults, and supports a mixture of global and tract-specific relations between WM and cortical GM change.

Supporting Information

S1 File. Supplementary results. Supplementary description of results depicted in Figs 2 and 4. (PDF)

Acknowledgments

The authors would like to thank Hilde W. Aasland, Claudia Nyberg, and Knut Overbye for their help with data collection for the present study.

Author Contributions

Conceived and designed the experiments: ABS AMF KBW. Performed the experiments: ABS AMF AY KBW. Analyzed the data: ABS. Contributed reagents/materials/analysis tools: AY. Wrote the paper: ABS AMF KBW.

References

1. Conforti L, Gilley J, Coleman MP. Wallerian degeneration: an emerging axon death pathway linking injury and disease. Nature reviews Neuroscience. 2014; 15(6):394–409. doi: 10.1038/nrn3680 PMID: 24840802.
2. Waller A. Experiments on the section of the glossopharyngeal and hypoglossal nerves of the frog, and observations of the alterations produced thereby in the structure of their primitive fibres. Philosophical Transactions of the Royal Society of London 1850; 140:423–9.
3. De Stefano N, Matthews PM, Filippi M, Agosta F, De Luca M, Bartolozzi ML, et al. Evidence of early cortical atrophy in MS: relevance to white matter changes and disability. Neurology. 2003; 60(7):1157–62. PMID: 12682324.
4. Mesulam M. The evolving landscape of human cortical connectivity: facts and inferences. NeuroImage. 2012; 62(4):2182–9. doi: 10.1016/j.neuroimage.2011.12.033 PMID: 22209814; PubMed Central PMCID: PMC3321392.
5. Fjell AM, Westlye LT, Amlien I, Espeseth T, Reinvang I, Raz N, et al. High consistency of regional cortical thinning in aging across multiple samples. Cerebral cortex. 2009; 19(9):2001–12. doi: 10.1093/cercor/bhn232 PMID: 19150922; PubMed Central PMCID: PMC2733683.
6. Walhovd KB, Westlye LT, Amlien I, Espeseth T, Reinvang I, Raz N, et al. Consistent neuroanatomical age-related volume differences across multiple samples. Neurobiology of aging. 2011; 32(5):916–32. doi: 10.1016/j.neurobiolaging.2009.05.013 PMID: 19570593.
7. Fjell AM, McEvoy L, Holland D, Dale AM, Walhovd KB, Alzheimer's Disease Neuroimaging I. Brain changes in older adults at very low risk for Alzheimer's disease. The Journal of neuroscience: the

official journal of the Society for Neuroscience. 2013; 33(19):8237–42. doi: 10.1523/JNEUROSCI.5506-12.2013 PMID: 23658162.

8. Pfefferbaum A, Rohlfing T, Rosenbloom MJ, Chu W, Colrain IM, Sullivan EV. Variation in longitudinal trajectories of regional brain volumes of healthy men and women (ages 10 to 85 years) measured with atlas-based parcellation of MRI. NeuroImage. 2013; 65:176–93. Epub 2012/10/16. doi: 10.1016/j.neuroimage.2012.10.008 PMID: 23063452; PubMed Central PMCID: PMC3516371.
9. Raz N, Ghisletta P, Rodrigue KM, Kennedy KM, Lindenberger U. Trajectories of brain aging in middle-aged and older adults: regional and individual differences. NeuroImage. 2010; 51(2):501–11. Epub 2010/03/20. doi: 10.1016/j.neuroimage.2010.03.020 PMID: 20298790; PubMed Central PMCID: PMC2879584.
10. Resnick SM, Pham DL, Kraut MA, Zonderman AB, Davatzikos C. Longitudinal magnetic resonance imaging studies of older adults: a shrinking brain. The Journal of neuroscience: the official journal of the Society for Neuroscience. 2003; 23(8):3295–301. PMID: 12716936.
11. Fjell AM, Walhovd KB, Fennema-Notestine C, McEvoy LK, Hagler DJ, Holland D, et al. One-year brain atrophy evident in healthy aging. J Neurosci. 2009; 29(48):15223–31. Epub 2009/12/04. doi: 10.1523/JNEUROSCI.3252-09.2009 PMID: 19955375; PubMed Central PMCID: PMC2827793.
12. Storsve AB, Fjell AM, Tamnes CK, Westlye LT, Overbye K, Aasland HW, et al. Differential Longitudinal Changes in Cortical Thickness, Surface Area and Volume across the Adult Life Span: Regions of Accelerating and Decelerating Change. The Journal of Neuroscience. 2014; 34(25):8488–98. doi: 10.1523/jneurosci.0391-14.2014 PMID: 24948804
13. Sexton CE, Walhovd KB, Storsve AB, Tamnes CK, Westlye LT, Johansen-Berg H, et al. Accelerated Changes in White Matter Microstructure during Aging: A Longitudinal Diffusion Tensor Imaging Study. The Journal of Neuroscience. 2014; 34(46):15425–36. doi: 10.1523/jneurosci.0203-14.2014 PMID: 25392509
14. Westlye LT, Walhovd KB, Dale AM, Bjornerud A, Due-Tonnessen P, Engvig A, et al. Differentiating maturational and aging-related changes of the cerebral cortex by use of thickness and signal intensity. NeuroImage. 2010; 52(1):172–85. doi: 10.1016/j.neuroimage.2010.03.056 PMID: 20347997.
15. Westlye LT, Walhovd KB, Dale AM, Bjornerud A, Due-Tonnessen P, Engvig A, et al. Life-span changes of the human brain white matter: diffusion tensor imaging (DTI) and volumetry. Cerebral cortex. 2010; 20(9):2055–68. doi: 10.1093/cercor/bhp280 PMID: 20032062.
16. Hogstrom LJ, Westlye LT, Walhovd KB, Fjell AM. The Structure of the Cerebral Cortex Across Adult Life: Age-Related Patterns of Surface Area, Thickness, and Gyrification. Cerebral cortex. 2012. Epub 2012/08/16. doi: 10.1093/cercor/bhs231 PMID: 22892423.
17. Walhovd KB, Westlye LT, Amlien I, Espeseth T, Reinvang I, Raz N, et al. Consistent neuroanatomical age-related volume differences across multiple samples. Neurobiol Aging. 2011; 32(5):916–32. Epub 2009/07/03. doi: 10.1016/j.neurobiolaging.2009.05.013 PMID: 19570593.
18. Fjell AM, Walhovd KB, Westlye LT, Ostby Y, Tamnes CK, Jernigan TL, et al. When does brain aging accelerate? Dangers of quadratic fits in cross-sectional studies. NeuroImage. 2010; 50(4):1376–83. Epub 2010/01/30. doi: 10.1016/j.neuroimage.2010.01.061 PMID: 20109562.
19. Callaghan MF, Freund P, Draganski B, Anderson E, Cappelletti M, Chowdhury R, et al. Widespread age-related differences in the human brain microstructure revealed by quantitative magnetic resonance imaging. Neurobiology of aging. 2014; 35(8):1862–72. doi: 10.1016/j.neurobiolaging.2014.02.008 PMID: 24656835; PubMed Central PMCID: PMC4024196.
20. Chetelat G, Landeau B, Salmon E, Yakushev I, Bahri MA, Mezenge F, et al. Relationships between brain metabolism decrease in normal aging and changes in structural and functional connectivity. NeuroImage. 2013; 76:167–77. doi: 10.1016/j.neuroimage.2013.03.009 PMID: 23518010.
21. Yendiki A, Panneck P, Srinivasan P, Stevens A, Zollei L, Augustinack J, et al. Automated probabilistic reconstruction of white-matter pathways in health and disease using an atlas of the underlying anatomy. Frontiers in neuroinformatics. 2011; 5:23. doi: 10.3389/fninf.2011.00023 PMID: 22016733; PubMed Central PMCID: PMC3193073.
22. Yendiki A, Reuter M, Wilkens P, Rosas HD, Fischl B. Joint reconstruction of white-matter pathways from longitudinal diffusion MRI data with anatomical priors. NeuroImage. 2016; 127:277–86. doi: http://dx.doi.org/10.1016/j.neuroimage.2015.12.003 PMID: 26717853
23. Bennett IJ, Madden DJ. Disconnected aging: Cerebral white matter integrity and age-related differences in cognition. Neuroscience. 2014; 276C:187–205. doi: 10.1016/j.neuroscience.2013.11.026 PMID: 24280637; PubMed Central PMCID: PMC4032380.
24. Penke L, Munoz Maniega S, Murray C, Gow AJ, Hernandez MC, Clayden JD, et al. A general factor of brain white matter integrity predicts information processing speed in healthy older people. The Journal of neuroscience: the official journal of the Society for Neuroscience. 2010; 30(22):7569–74. doi: 10.1523/JNEUROSCI.1553-10.2010 PMID: 20519531.

25. Li YO, Yang FG, Nguyen CT, Cooper SR, LaHue SC, Venugopal S, et al. Independent component analysis of DTI reveals multivariate microstructural correlations of white matter in the human brain. Human brain mapping. 2012; 33(6):1431–51. doi: 10.1002/hbm.21292 PMID: 21567660.

26. Lovden M, Laukka EJ, Rieckmann A, Kalpouzos G, Li TQ, Jonsson T, et al. The dimensionality of between-person differences in white matter microstructure in old age. Human brain mapping. 2013; 34 (6):1386–98. doi: 10.1002/hbm.21518 PMID: 22331619.

27. Johnson MA, Diaz MT, Madden DJ. Global versus tract-specific components of cerebral white matter integrity: relation to adult age and perceptual-motor speed. Brain structure & function. 2014. doi: 10.1007/s00429-014-0822-9 PMID: 24972959.

28. Agosta F, Pievani M, Sala S, Geroldi C, Galluzzi S, Frisoni GB, et al. White matter damage in Alzheimer disease and its relationship to gray matter atrophy. Radiology. 2011; 258(3):853–63. doi: 10.1148/radiol.10101284 PMID: 21177393.

29. Salat DH, Tuch DS, Greve DN, van der Kouwe AJ, Hevelone ND, Zaleta AK, et al. Age-related alterations in white matter microstructure measured by diffusion tensor imaging. Neurobiology of aging. 2005; 26(8):1215–27. Epub 2005/05/27. doi: 10.1016/j.neurobiolaging.2004.09.017 PMID: 15917106.

30. Maillard P, Carmichael O, Harvey D, Fletcher E, Reed B, Mungas D, et al. FLAIR and diffusion MRI signals are independent predictors of white matter hyperintensities. AJNR Am J Neuroradiol. 2013; 34 (1):54–61. Epub 2012/06/16. doi: 10.3174/ajnr.A3146 PMID: 22700749; PubMed Central PMCID: PMCPmc3710440.

31. Bosch B, Arenaza-Urquijo EM, Rami L, Sala-Llonch R, Junque C, Sole-Padulles C, et al. Multiple DTI index analysis in normal aging, amnestic MCI and AD. Relationship with neuropsychological performance. Neurobiology of aging. 2012; 33(1):61–74. doi: 10.1016/j.neurobiolaging.2010.02.004 PMID: 20371138.

32. Amlien IK, Fjell AM. Diffusion tensor imaging of white matter degeneration in Alzheimer's disease and mild cognitive impairment. Neuroscience. 2014; 276C:206–15. doi: 10.1016/j.neuroscience.2014.02.017 PMID: 24583036.

33. Collins-Praino LE, Francis YI, Griffith EY, Wiegman AF, Urbach J, Lawton A, et al. Soluble amyloid beta levels are elevated in the white matter of Alzheimer's patients, independent of cortical plaque severity. Acta neuropathologica communications. 2014; 2:83. doi: 10.1186/PREACCEPT-3091772881321882 PMID: 25129614; PubMed Central PMCID: PMC4147157.

34. Walhovd KB, Storsve AB, Westlye LT, Drevon CA, Fjell AM. Blood markers of fatty acids and vitamin D, cardiovascular measures, body mass index, and physical activity relate to longitudinal cortical thinning in normal aging. Neurobiology of Aging. 2014; 35(5):1055–64. doi: http://dx.doi.org/10.1016/j.neurobiolaging.2013.11.011 PMID: 24332985

35. Folstein MF, Folstein SE, McHugh PR. ‚ÄúMini-mental state‚Äù: A practical method for grading the cognitive state of patients for the clinician. Journal of Psychiatric Research. 1975; 12(3):189–98. http://dx.doi.org/10.1016/0022-3956(75)90026-6. PMID: 1202204

36. Beck AT, Steer R. Beck depression inventory scoring manual: New York: The Psychological Corporation; 1987.

37. Wechsler D. Wechsler abbreviated scale of intelligence: The Psychological Corporation, San Antonio, TX; 1999.

38. Delis DC, Kramer JH, Kaplan E, Ober BA. California Verbal Learning Test—Second Edition (CVLT—II): The Psychological Corporation, San Antonio, TX; 2000.

39. Narr KL, Woods RP, Thompson PM, Szeszko P, Robinson D, Dimtcheva T, et al. Relationships between IQ and Regional Cortical Gray Matter Thickness in Healthy Adults. Cerebral Cortex. 2007; 17 (9):2163–71. doi: 10.1093/cercor/bhl125 PMID: 17118969

40. Schnack HG, van Haren NEM, Brouwer RM, Evans A, Durston S, Boomsma DI, et al. Changes in Thickness and Surface Area of the Human Cortex and Their Relationship with Intelligence. Cerebral Cortex. 2014. doi: 10.1093/cercor/bht357

41. Navas-Sánchez FJ, Alemán-Gómez Y, Sánchez-Gonzalez J, Guzmán-De-Villoria JA, Franco C, Robles O, et al. White matter microstructure correlates of mathematical giftedness and intelligence quotient. Human Brain Mapping. 2014; 35(6):2619–31. doi: 10.1002/hbm.22355 PMID: 24038774

42. Reese TG, Heid O, Weisskoff RM, Wedeen VJ. Reduction of eddy-current-induced distortion in diffusion MRI using a twice-refocused spin echo. Magn Reson Med. 2003; 49(1):177–82. Epub 2003/01/02. doi: 10.1002/mrm.10308 PMID: 12509835.

43. Jovicich J, Czanner S, Greve D, Haley E, van der Kouwe A, Gollub R, et al. Reliability in multi-site structural MRI studies: effects of gradient non-linearity correction on phantom and human data. NeuroImage. 2006; 30:436–43. doi: 10.1016/j.neuroimage.2005.09.046 PMID: 16300968.

44. Sled JG, Zijdenbos AP, Evans AC. A nonparametric method for automatic correction of intensity nonuniformity in MRI data. IEEE Trans Med Imaging. 1998; 17:87–97. doi: 10.1109/42.668698 PMID: 9617910.

45. Fischl B, Salat DH, Busa E, Albert M, Dieterich M, Haselgrove C, et al. Whole brain segmentation: automated labeling of neuroanatomical structures in the human brain. Neuron. 2002; 33:341–55. PMID: 11832223.

46. Dale AM, Fischl B, Sereno MI. Cortical surface-based analysis. I. Segmentation and surface reconstruction. NeuroImage. 1999; 9:179–94. doi: 10.1006/nimg.1998.0395 PMID: 9931268.

47. Fischl B, Sereno MI, Dale AM. Cortical surface-based analysis. II: Inflation, flattening, and a surface-based coordinate system. NeuroImage. 1999; 9:195–207. doi: 10.1006/nimg.1998.0396 PMID: 9931269.

48. Fischl B, Dale AM. Measuring the thickness of the human cerebral cortex from magnetic resonance images. Proc Natl Acad Sci U S A. 2000; 97:11050–5. doi: 10.1073/pnas.200033797 PMID: 10984517; PubMed Central PMCID: PMC27146.

49. Fischl B, van der Kouwe A, Destrieux C, Halgren E, Segonne F, Salat DH, et al. Automatically parcellating the human cerebral cortex. Cereb Cortex. 2004; 14:11–22. PMID: 14654453.

50. Desikan RS, Segonne F, Fischl B, Quinn BT, Dickerson BC, Blacker D, et al. An automated labeling system for subdividing the human cerebral cortex on MRI scans into gyral based regions of interest. NeuroImage. 2006; 31:968–80. doi: 10.1016/j.neuroimage.2006.01.021 PMID: 16530430.

51. Reuter M, Schmansky NJ, Rosas HD, Fischl B. Within-subject template estimation for unbiased longitudinal image analysis. NeuroImage. 2012; 61(4):1402–18. doi: http://dx.doi.org/10.1016/j.neuroimage.2012.02.084 PMID: 22430496

52. Reuter M, Rosas HD, Fischl B. Highly accurate inverse consistent registration: A robust approach. NeuroImage. 2010; 53(4):1181–96. doi: http://dx.doi.org/10.1016/j.neuroimage.2010.07.020 PMID: 20637289

53. Reuter M, Fischl B. Avoiding asymmetry-induced bias in longitudinal image processing. NeuroImage. 2011; 57(1):19–21. doi: http://dx.doi.org/10.1016/j.neuroimage.2011.02.076 PMID: 21376812

54. Thompson WK, Holland D. Bias in tensor based morphometry Stat-ROI measures may result in unrealistic power estimates. NeuroImage. 2011; 57(1):1–4. doi: http://dx.doi.org/10.1016/j.neuroimage.2010.11.092 PMID: 21349340

55. Fischl B, Sereno MI, Tootell RBH, Dale AM. High-resolution intersubject averaging and a coordinate system for the cortical surface. Human brain mapping. 1999; 8(4):272–84. doi: 10.1002/(sici)1097-0193(1999)8:4<272::aid-hbm10>3.0.co;2–4 PMID: 10619420

56. Jenkinson M, Bannister P, Brady M, Smith S. Improved optimization for the robust and accurate linear registration and motion correction of brain images. NeuroImage. 2002; 17(2):825–41. PMID: 12377157.

57. Rohde GK, Barnett AS, Basser PJ, Marenco S, Pierpaoli C. Comprehensive approach for correction of motion and distortion in diffusion-weighted MRI. Magnetic resonance in medicine: official journal of the Society of Magnetic Resonance in Medicine / Society of Magnetic Resonance in Medicine. 2004; 51(1):103–14. doi: 10.1002/mrm.10677 PMID: 14705050.

58. Leemans A, Jones DK. The B-matrix must be rotated when correcting for subject motion in DTI data. Magnetic resonance in medicine: official journal of the Society of Magnetic Resonance in Medicine / Society of Magnetic Resonance in Medicine. 2009; 61(6):1336–49. doi: 10.1002/mrm.21890 PMID: 19319973.

59. Greve DN, Fischl B. Accurate and robust brain image alignment using boundary-based registration. NeuroImage. 2009; 48(1):63–72. doi: 10.1016/j.neuroimage.2009.06.060 PMID: 19573611; PubMed Central PMCID: PMC2733527.

60. Behrens TE, Berg HJ, Jbabdi S, Rushworth MF, Woolrich MW. Probabilistic diffusion tractography with multiple fibre orientations: What can we gain? NeuroImage. 2007; 34(1):144–55. doi: 10.1016/j.neuroimage.2006.09.018 PMID: 17070705.

61. Yendiki A, Koldewyn K, Kakunoori S, Kanwisher N, Fischl B. Spurious group differences due to head motion in a diffusion MRI study. NeuroImage. 2013; 88C:79–90. doi: 10.1016/j.neuroimage.2013.11.027 PMID: 24269273; PubMed Central PMCID: PMC4029882.

62. Benner T, van der Kouwe AJ, Sorensen AG. Diffusion imaging with prospective motion correction and reacquisition. Magnetic resonance in medicine: official journal of the Society of Magnetic Resonance in Medicine / Society of Magnetic Resonance in Medicine. 2011; 66(1):154–67. doi: 10.1002/mrm.22837 PMID: 21695721; PubMed Central PMCID: PMC3121006.

63. Hagler DJ Jr, Saygin AP, Sereno MI. Smoothing and cluster thresholding for cortical surface-based group analysis of fMRI data. NeuroImage. 2006; 33(4):1093–103. http://dx.doi.org/10.1016/j.neuroimage.2006.07.036. PMID: 17011792

64. Hayasaka S, Nichols TE. Validating cluster size inference: random field and permutation methods. NeuroImage. 2003; 20(4):2343–56. http://dx.doi.org/10.1016/j.neuroimage.2003.08.003. PMID: 14683734

65. Bennett IJ, Madden DJ, Vaidya CJ, Howard DV, Howard JH. Age-related differences in multiple measures of white matter integrity: A diffusion tensor imaging study of healthy aging. Human Brain Mapping. 2010; 31(3):378–90. doi: 10.1002/hbm.20872 PMID: 19662658

66. Bartzokis G, Lu PH, Heydari P, Couvrette A, Lee GJ, Kalashyan G, et al. Multimodal Magnetic Resonance Imaging Assessment of White Matter Aging Trajectories Over the Lifespan of Healthy Individuals. Biological Psychiatry. 2012; 72(12):1026–34. doi: http://dx.doi.org/10.1016/j.biopsych.2012.07.010 PMID: 23017471

67. Barrick TR, Charlton RA, Clark CA, Markus HS. White matter structural decline in normal ageing: A prospective longitudinal study using tract-based spatial statistics. NeuroImage. 2010; 51(2):565–77. doi: 10.1016/j.neuroimage.2010.02.033 PMID: 20178850

68. Sullivan EV, Rohlfing T, Pfefferbaum A. Quantitative fiber tracking of lateral and interhemispheric white matter systems in normal aging: Relations to timed performance. Neurobiology of Aging. 2010; 31(3):464–81. doi: http://dx.doi.org/10.1016/j.neurobiolaging.2008.04.007 PMID: 18495300

69. Burzynska AZ, Preuschhof C, Bäckman L, Nyberg L, Li SC, Lindenberger U, et al. Age-related differences in white matter microstructure: Region-specific patterns of diffusivity. NeuroImage. 2010; 49(3):2104–12. doi: http://dx.doi.org/10.1016/j.neuroimage.2009.09.041 PMID: 19782758

70. Yap Q, Teh I, Fusar-Poli P, Sum M, Kuswanto C, Sim K. Tracking cerebral white matter changes across the lifespan: insights from diffusion tensor imaging studies. J Neural Transm. 2013; 120(9):1369–95. doi: 10.1007/s00702-013-0971-7 PMID: 23328950

71. Head D, Buckner RL, Shimony JS, Williams LE, Akbudak E, Conturo TE, et al. Differential Vulnerability of Anterior White Matter in Nondemented Aging with Minimal Acceleration in Dementia of the Alzheimer Type: Evidence from Diffusion Tensor Imaging. Cerebral Cortex. 2004; 14(4):410–23. doi: 10.1093/cercor/bhh003 PMID: 15028645

72. Sullivan EV, Zahr NM, Rohlfing T, Pfefferbaum A. Fiber tracking functionally distinct components of the internal capsule. Neuropsychologia. 2010; 48(14):4155–63. doi: http://dx.doi.org/10.1016/j.neuropsychologia.2010.10.023 PMID: 20974161

73. Colby JB, Van Horn JD, Sowell ER. Quantitative in vivo evidence for broad regional gradients in the timing of white matter maturation during adolescence. NeuroImage. 2011; 54(1):25–31. doi: http://dx.doi.org/10.1016/j.neuroimage.2010.08.014 PMID: 20708693

74. Raz N. Ageing and the Brain. eLS: John Wiley & Sons, Ltd; 2001.

75. Kucyi A, Moayedi M, Weissman-Fogel I, Hodaie M, Davis KD. Hemispheric Asymmetry in White Matter Connectivity of the Temporoparietal Junction with the Insula and Prefrontal Cortex. PLoS ONE. 2012; 7(4):e35589. doi: 10.1371/journal.pone.0035589 PMID: 22536413

76. Terry RD, DeTeresa R, Hansen LA. Neocortical cell counts in normal human adult aging. Annals of neurology. 1987; 21(6):530–9. doi: 10.1002/ana.410210603 PMID: 3606042.

77. Peters A, Morrison JH, Rosene DL, Hyman BT. Feature article: are neurons lost from the primate cerebral cortex during normal aging? Cerebral cortex. 1998; 8(4):295–300. PMID: 9651126.

78. Freeman SH, Kandel R, Cruz L, Rozkalne A, Newell K, Frosch MP, et al. Preservation of neuronal number despite age-related cortical brain atrophy in elderly subjects without Alzheimer disease. Journal of neuropathology and experimental neurology. 2008; 67(12):1205–12. doi: 10.1097/NEN.0b013e31818fc72f PMID: 19018241; PubMed Central PMCID: PMC2734185.

79. Esiri MM. Ageing and the brain. The Journal of pathology. 2007; 211(2):181–7. doi: 10.1002/path.2089 PMID: 17200950.

80. Ramcharitar J, Afonso VM, Albrecht S, Bennett DA, LeBlanc AC. Caspase-6 activity predicts lower episodic memory ability in aged individuals. Neurobiology of aging. 2013; 34(7):1815–24. doi: 10.1016/j.neurobiolaging.2013.01.007 PMID: 23402898; PubMed Central PMCID: PMC3772349.

81. Forkel SJ, Thiebaut de Schotten M, Kawadler JM, Dell'Acqua F, Danek A, Catani M. The anatomy of fronto-occipital connections from early blunt dissections to contemporary tractography. Cortex; a journal devoted to the study of the nervous system and behavior. 2014; 56:73–84. doi: 10.1016/j.cortex.2012.09.005 PMID: 23137651.

82. Vergani F, Mahmood S, Morris CM, Mitchell P, Forkel SJ. Intralobar fibres of the occipital lobe: a post mortem dissection study. Cortex; a journal devoted to the study of the nervous system and behavior. 2014; 56:145–56. doi: 10.1016/j.cortex.2014.03.002 PMID: 24768339.

83. Ehrlich S, Geisler D, Yendiki A, Panneck P, Roessner V, Calhoun VD, et al. Associations of White Matter Integrity and Cortical Thickness in Patients With Schizophrenia and Healthy Controls. Schizophrenia Bulletin. 2014; 40(3):665–74. doi: 10.1093/schbul/sbt056 PMID: 23661633

84. Phillips OR, Clark KA, Woods RP, Subotnik KL, Asarnow RF, Nuechterlein KH, et al. Topographical relationships between arcuate fasciculus connectivity and cortical thickness. Human brain mapping. 2011; 32(11):1788–801. Epub 2010/10/05. doi: 10.1002/hbm.21147 PMID: 20886580; PubMed Central PMCID: PMC3071430.

85. Bodini B, Khaleeli Z, Cercignani M, Miller DH, Thompson AJ, Ciccarelli O. Exploring the relationship between white matter and gray matter damage in early primary progressive multiple sclerosis: An in vivo study with TBSS and VBM. Human Brain Mapping. 2009; 30(9):2852–61. doi: 10.1002/hbm.20713 PMID: 19172648

86. Sexton CE, Storsve AB, Walhovd KB, Johansen-Berg H, Fjell AM. Poor sleep quality is associated with increased cortical atrophy in community-dwelling adults. Neurology. 2014; 83(11):967–73. doi: 10.1212/WNL.0000000000000774 PMID: 25186857.

87. Smith AD, Smith SM, de Jager CA, Whitbread P, Johnston C, Agacinski G, et al. Homocysteine-lowering by B vitamins slows the rate of accelerated brain atrophy in mild cognitive impairment: a randomized controlled trial. PloS one. 2010; 5(9):e12244. Epub 2010/09/15. doi: 10.1371/journal.pone.0012244 PMID: 20838622; PubMed Central PMCID: PMC2935890.

88. Walhovd KB, Storsve AB, Westlye LT, Drevon CA, Fjell AM. Blood markers of fatty acids and vitamin D, cardiovascular measures, body mass index, and physical activity relate to longitudinal cortical thinning in normal aging. Neurobiology of aging. 2014; 35(5):1055–64. doi: 10.1016/j.neurobiolaging.2013.11.011 PMID: 24332985.

89. Thompson PM, Cannon TD, Narr KL, van Erp T, Poutanen VP, Huttunen M, et al. Genetic influences on brain structure. Nature neuroscience. 2001; 4(12):1253–8. doi: 10.1038/nn758 PMID: 11694885.

90. Brouwer RM, Hedman AM, van Haren NE, Schnack HG, Brans RG, Smit DJ, et al. Heritability of brain volume change and its relation to intelligence. NeuroImage. 2014; 100:676–83. doi: 10.1016/j.neuroimage.2014.04.072 PMID: 24816534.

91. Bender AR, Prindle JJ, Brandmaier AM, Raz N. White matter and memory in healthy adults: Coupled changes over two years. NeuroImage. http://dx.doi.org/10.1016/j.neuroimage.2015.10.085.